Phytoplankton photophysiology across subtropical eddies: deconvolving nutrient, light, and community signals

Haoran Liu[1, 2], Yuyuan Xie[1*], Thomas J. Browning[2], Feipeng Xu[1], Bangqin Huang[1*]

[1]Xiamen University, China, [2]GEOMAR Helmholtz Center for Ocean Research Kiel, Helmholtz Association of German Research Centres (HZ), Germany

Submitted to Journal:
Frontiers in Marine Science

Specialty Section:
Marine Biogeochemistry

Article type:
Original Research Article

Manuscript ID:
934391

Received on:
02 May 2022

Revised on:
16 Aug 2022

Journal website link:
www.frontiersin.org

Conflict of interest statement

The authors declare that the research was conducted in the absence of any commercial or financial relationships that could be construed as a potential conflict of interest

Author contribution statement

HL, YX and BH conceived this study. HL and FX conducted the sample collection and analysis. HL drafted the original manuscript. YX and TJB critically reviewed and edited the manuscript. All authors contributed to the article and approved the submitted version.

Keywords

Diel variation, Fast Repetition Rate Fluorometry, photoinhibition, nutrient limitation, South China Sea, eddy

Abstract

Word count: 206

Fast Repetition Rate fluorometry (FRRf) based on active chlorophyll fluorescence is a powerful, noninvasive tool for studying phytoplankton physiological status at high spatial and temporal resolution. The South China Sea (SCS) is one of the largest tropical-subtropical marginal seas in the world, which plays an important role in modulating regional carbon budget and climate. In this study, underway in-situ FRRf measurements were carried out throughout the outer continental shelf of the northern SCS, the basin of the northern SCS, the cyclonic eddy influenced domain in the western SCS, and the basin of the southeastern SCS. Pronounced diurnal variability of FRRf-derived parameters were observed, characterized by a large midday depression and slight nocturnal depression of the maximum quantum yield of photosystem II (Fv/Fm), and a slight increase in the functional absorption cross section of photosystem II photochemistry (σPSII) at noon. Fv/Fm at surface was typically as low as 0.1 – 0.3 and exhibited higher values (~0.4) where internal waves occurred. The cyclonic eddy increased Fv/Fm slightly implying it had a limited impact on surface phytoplankton photophysiology. With proper interpretation, FRRf has been a powerful tool to assess the physiological status of phytoplankton in the sea and to correlate that to ocean dynamics in an unprecedented fine scale.

Contribution to the field

Studies in mesoscale processes in the ocean demand high-resolution data. This manuscript reports a high-resolution measurement of phytoplankton physiology in the South China Sea in areas of both cyclonic and anti-cyclonic eddies. Deconvolution of multi-factors extracted a clearer picture of phytoplankton having consistently more active physiological status inside cyclonic eddies.

Funding statement

This work was supported by the National Natural Science Foundation of China through grants 42130401 and 42141002.

Ethics statements

Studies involving animal subjects

Generated Statement: No animal studies are presented in this manuscript.

Studies involving human subjects

Generated Statement: No human studies are presented in this manuscript.

Inclusion of identifiable human data

Generated Statement: No potentially identifiable human images or data is presented in this study.

Data availability statement

Generated Statement: The raw data supporting the conclusions of this article will be made available by the authors, without undue reservation.

Phytoplankton photophysiology across subtropical eddies: deconvolving nutrient, light, and community signals

Haoran Liu[1,2], Yuyuan Xie[1,3*], Thomas J. Browning[2], Feipeng Xu[1], Bangqin Huang[1*]

[1]State Key Laboratory of Marine Environmental Science, Fujian Provincial Key Laboratory of Coastal Ecology and Environmental Studies, Xiamen University, Xiamen, Fujian, China

[2]GEOMAR Helmholtz Centre for Ocean Research Kiel, Kiel, Germany

[3]Current address: College of Marine Science, University of South Florida, St. Petersburg, FL, USA

*** Correspondence:**
Yuyuan Xie,
xieyuyuan@hotmail.com;
Bangqin Huang,
bqhuang@xmu.edu.cn

Keywords: Diel variation, Fast Repetition Rate fluorometry, Eddy, Photoinhibition, Nutrient limitation, South China Sea.

Abstract

Fast Repetition Rate fluorometry (FRRf) based on active chlorophyll fluorescence is a powerful, noninvasive tool for studying phytoplankton physiological status at high spatial and temporal resolution. The South China Sea (SCS) is one of the largest tropical-subtropical marginal seas in the world, which plays an important role in modulating regional carbon budget and climate. In this study, underway in-situ FRRf measurements were carried out throughout the outer continental shelf of the northern SCS, the basin of the northern SCS, the cyclonic eddy influenced domain in the western SCS, and the basin of the southeastern SCS. Pronounced diurnal variability of FRRf-derived parameters were observed, characterized by a large midday depression and slight nocturnal depression of the maximum quantum yield of photosystem II (F_v/F_m), and a slight increase in the functional absorption cross section of photosystem II photochemistry (σ_{PSII}) at noon. F_v/F_m at surface was typically as low as 0.1 – 0.3 and exhibited higher values (~0.4) where internal waves occurred. The cyclonic eddy increased F_v/F_m slightly implying it had a limited impact on surface phytoplankton photophysiology. With proper interpretation, FRRf has been a powerful tool to assess the physiological status of phytoplankton in the sea and to correlate that to ocean dynamics in an unprecedented fine scale.

1 Introduction

Phytoplankton account for around half of global primary production (PP) and play an important role in regulating carbon cycling and climate (Field et al., 1998; Longhurst et al., 1995; Falkowski et al., 1998). In contrast to conventional methods requiring water sampling and incubation (e.g., incubation with ^{14}C tracer), Fast Repetition Rate fluorometry (FRRf) (Kolber et al., 1998) is an active chlorophyll-*a* (Chl*a*) fluorescence technique rapidly probing phytoplankton physiological and bio-optical parameters in-situ (Kolber and Falkowski, 1993; Behrenfeld and Kolber, 1999; Behrenfeld et al., 2006; Suggett et al., 2009; Schuback and Tortell, 2019; Zhu et al., 2022). There is significant

potential to use FRRf signals to extend observations to much finer spatial and temporal scales than achievable with conventional techniques (Hughes et al. 2018). However, FRRf-derived signals are the result of the interacting influence of both the phytoplankton communities present and their physiological status, which in turn is impacted by environmental forcing (Suggett et al., 2009; Behrenfeld and Milligan, 2013). Their interpretation is therefore not always straightforward and there is a need for more studies measuring ancillary biological and environmental parameters alongside FRRf in order to deconvolve these signals (Suggett et al., 2009; Behrenfeld and Milligan, 2013).

Phytoplankton growth in the ocean is frequently limited by nutrient availability, particularly in the sunlit surface waters of the low latitude oceans (Moore et al., 2013). Chlorophyll fluorescence measured by FRRf appears to be highly sensitive to nutrient limitation status, with limitation by either iron (Fe) and/or nitrogen (N)—the main limiting nutrients in the current ocean (Moore et al., 2013)—strongly regulating FRRf-derived parameters (Behrenfeld and Milligan, 2013). Specifically, at dawn and dusk when non-photochemical quenching (NPQ) processes are relaxed, values of the maximum quantum yield of photosystem II (PSII), F_v/F_m, are typically elevated under low N conditions and depressed under elevated N, low Fe conditions (Behrenfeld et al., 2006; Moore et al., 2008; Browning et al., 2014). Furthermore, in the tropical oceans under conditions of low Fe in combination with either low or elevated N, F_v/F_m values have been observed to show night time decreases from dusk through to dawn (Behrenfeld and Kolber, 1999). This has been suggested to be due to cyanobacteria using their photosynthetic apparatus for respiratory electron transfer at night (Campbell et al., 1998), which under low Fe conditions leads to a strongly reduced plastoquinone (PQ) pool due to restricted availability of Fe-rich photosystem I and cytochrome b6f proteins relative to the lower Fe PSII (Behrenfeld et al., 2006; Schrader et al., 2011). Night time reductions of σ_{PSII} also reflect increased night time reduction of the PQ pool under low Fe conditions (Behrenfeld and Kolber, 1999). Conversely, under Fe replete, N limited conditions, nocturnal reductions in F_v/F_m and functional absorption cross section of PSII photochemistry (σ_{PSII}) are much smaller or absent (Behrenfeld et al., 2006). Therefore, in addition to discrete measurements of F_v/F_m and σ_{PSII} made at any given time point, diurnal patterns in continuous active chlorophyll fluorescence could provide rich information for mapping nutrient stress status; specifically, via distinguishing Fe, N or N-Fe (co-)limitations (Behrenfeld and Milligan, 2013).

Independent of nutrient limitation, changes in F_v/F_m can also be related to phytoplankton community structure, with smaller values of F_v/F_m linked to increased antenna size of PSII, which has been found to be the case for small eukaryotic phytoplankton relative to large species in laboratory cultures (Suggett et al., 2009). Furthermore, strong decreases in F_v/F_m are associated with elevated light levels (reflecting light intensity that exceeds photosynthetic demand) (Wei et al., 2020). The suit of mechanisms down-regulating F_v/F_m at elevated light levels are collectively termed non-photochemical quenching (NPQ), which can be reversed over timescales of seconds to hours upon exposure of phytoplankton to darkness (Falkowski and Raven, 2007).

The South China Sea (SCS) is the largest marginal sea of the North Pacific. Mesoscale physical processes, such as eddies, occur frequently in different parts of the SCS, significantly impacting nutrient distributions and carbon cycling (Xiu et al., 2010; Xiu and Chai, 2011; Jiao et al., 2014; Li et al., 2017; Zhang et al., 2020). These physical processes result in distinct patterns of phytoplankton community structure (Huang et al., 2010; Wang et al., 2016; Wang et al., 2018), PP (Ning et al., 2004; Liao et al., 2021), and supposedly physiology (Liao et al., 2021). Cyclonic eddies (CE) occur frequently during summer in the western SCS, driving a shoaling of the nitracline depth to as shallow as 20 m relative to ~70 m in the background state (Jiao et al., 2014). Chl*a* biomass of diatoms and *Synechococcus* alongside overall rates of PP have been observed to rise significantly inside CE as a

consequence of enhanced nutrient supply (Wang et al., 2016; Liao et al., 2021). In contrast, the effects of anticyclonic eddies (ACE) on phytoplankton community structure are more diverse, with ACE leading to convergence of low nutrient surface waters leading to the community structure inside ACE being similar to that of surrounding waters (Huang et al., 2010). In addition, sub-mesoscale upwelling at the edge of ACE have been shown to drive a modest effect of increasing the Chl*a* biomass of diatoms and haptophytes (Wang et al., 2018).

So far studies of eddies in the SCS have not been made accompanying measurements of photophysiology. However, other studies have indicated that nutrient availability impacts photophysiology in this region (Jin et al., 2016; Xie et al., 2018). Using diel FRRf measurements, Jin et al. (2016) investigated phytoplankton physiology at local noon in the northern SCS, showing decreasing F_v/F_m values from the coast to central basin and increasing values from the surface to deep. Furthermore, Xie et al. (2018) measured the diel cycle of F_v/F_m for a natural assemblage of *Prochlorococcus*, the most abundant phytoplankton class in the SCS, and related the observed diel variability to nutrient stress (Xie et al., 2018). Here, we undertook a FRRf survey over a much larger area of the SCS than in these previous studies, ranging from the outer continental shelf to the entire basin and crossing CE and ACE features, and complementing these measurements with diagnostic pigment analyses to aid with deconvolving nutrient, community and light effects on F_v/F_m and σ_{PSII}.

2 Materials and Methods

2.1 Underway FRRf measurements

Observations were made during cruise KK1808 onboard the R/V Tan *Kah Kee* (18th September –14th October 2018). Underway FRRf measurements were conducted with a FastOcean coupled with an Act2 Laboratory System (Chelsea Technologies, UK). The ship's underway system collected seawater continuously from a depth of ~5 m which then transitioned through a ~50 m dark pipe before flowing into the Act2 System. The dark acclimation period from water entering the vessel through to FRRf measurement was estimated to last around 5 minutes, which is similar to the Behrenfeld and Kolber et al. (1999). The FRRf was set to perform acquisitions using 100 blue excitation (450 nm) flashlets with 2 microseconds intervals. Fluorescence transients were fit within the manufacturers software (ActRun) to yield the initial fluorescence yield (F_o), maximum fluorescence yield (F_m) and σ_{PSII}. Blank fluorescence of deionized water (Milli-Q) samples was subtracted from raw F_o and F_m values and F_v/F_m recalculated.

2.2 Continuous shipboard measurements and satellite data products

Time and geographic coordinates were recorded by the shipboard geographical positioning system (GPS). The time was converted to local time, allowing alignment of light-dark periods. Sea-surface temperature (SST) and salinity were continuously measured by a SBE21 CTD (Sea-Bird Electronics, USA). The FastOcean plus Act2 Laboratory System measured fluorescence-based Chlorophyll *a* concentrations (Chla^{FRRf}), which was then calibrated against HPLC-determined concentrations of Chlorophyll *a* pigments. To characterize the mesoscale eddies in the study area, daily, 1/4° gridded sea level anomaly (SLA) data between 8th September and 14th October 2018 were downloaded from the Copernicus Marine and Environment Monitoring Service (CMEMS) (available from: http://marine.copernicus.eu/). In addition, 10-minute resolution instantaneous photosynthetically available radiation (iPAR, μmol quanta m^{-2} s^{-1}) was extracted from Himawari-8 level 2 products (available from: https://www.eorc.jaxa.jp/ptree/), and daily integrated surface PAR data (mol quanta m^{-2} d^{-1}) was extracted from the standard MODIS-Aqua Level-3 products at 4-km pixel resolution (available from: http://oceancolor.gsfc.nasa.gov/). Each in situ underway measurement were matched

with a daily SLA, iPAR, and PAR dataset using the closest pixel of the respective satellite products. Himawari-8 derived iPAR values were consistent with in-situ measurement derived from PAR sensor mounted in the CTD with p <0.01 and r =0.87 (Fig. S1).

2.3 Pigments and Chemotaxonomic Analysis

Seawater samples were collected with Niskin bottles from discrete depths at stations (Fig. 1). Seawater (4–16 L) at each depth was filtered onto a 47 mm diameter GF/F glass fiber filter under gentle vacuum (<150 mmHg) and stored in liquid nitrogen until analysis. In the laboratory, filters were immersed in N, N-dimethylformamide for pigment extraction. Extracts were analyzed with an UltiMate 3000 High Performance Liquid Chromatography (HPLC) system (ThermoFisher Scientific, USA) calibrated with pigment standards (DHI Water & Environment, Denmark) following the procedure of Furuya et al. (2003).

Thirteen pigments detected included chlorophyll *c*2, chlorophyll *c*3, peridinin, 19'-butanoyloxyfucoxanthin, fucoxanthin, neoxanthin, prasinoxanthin, 19'-hexanoyloxyfucoxanthin, violaxanthin, diadinoxanthin, alloxanthin, diatoxanthin, zeaxanthin, lutein, chlorophyll *a*, chlorophyll *b*, divinyl chlorophyll *a*, *α*-carotene, and *β*-carotene. CHEMTAX software was then used to estimate the contribution of different phytoplankton types to total chlorophyll *a* (the sum of chlorophyll *a* and divinyl chlorophyll *a*) (Mackey et al., 1996). The initial input matrix of ratios of diagnostic pigments to total chlorophyll *a* was identical to the input matrix used in previous studies in the South China Sea (Wang et al. 2015; Xiao et al., 2018). Successive runs were done for each group to gain convergence between input and output ratios according to the CHEMTAX protocols described by Latasa (2007). Nine phytoplankton classes were computed, including Dinoflagellates (Dino), Diatoms (Diat), Type-8 Haptophytes (Hapt_8), Type-6 Haptophytes (Hapt_6), Cryptophytes (Cryp), Chlorophytes (Chlo), Prasinophytes (Pras), *Synechococcus* (*Syne*), and *Prochlorococcus* (*Proc*), and we used only surface phytoplankton information in this study. In addition, the carotenoids were separated into photosynthetic carotenoids (PSCs) and photo-protective carotenoids (PPCs). The former includes Peridinin, 19'-Butanoyloxyfucoxanth, Fucoxanthin, and 19'-Hexanoyloxyfucoxanthin. The latter includes violaxanthin, diadinoxanthin, alloxanthin, diatoxanthin, zeaxanthin, ββ- + βε-carotene, and Lutein (Barlow et al., 2007).

2.4 Statistical analysis

Pearson's correlation coefficient (r) was used to assess for correlations across the dataset. A one-way ANOVA was used for statistical analysis to compare the difference between environmental and FRRf-dervied parameters among sections. In order to deconvolve light signal and other factors for F_v/F_m, a simple model was constructed. In the model, F_v/F_m is a linear function of iPAR, and the constant of the linear function represents influence of other factors together, but different regions have different constants for their own nutrient conditions; in addition, a two-way ANOVA was conducted in the beginning and determined that both light and region were significant factors and the slope of the linear function is invariant for different regions (because of no interaction effect between light and region, Table S1). All statistical analyses were performed using open source statistical software R version 3.6.0 (R Development Core Team, 2016). Figures were plotted using Ocean Data View 5 (Schlitzer, 2019) and R software.

3 Results

Clear variations in hydrographic properties and SLA during the cruise were observed (Figs. 1 and 2). Chlorophyll fluorescence was relatively elevated in the northern SCS continental shelf transect

selected as S1; relative lower SST and higher salinity was observed around 18° SCS and was named S2; SLA images identified the positions of one cyclonic eddy (CE) and two anticyclonic eddies (ACEs, ACE1 and ACE2) that our cruise passed through; accordingly we then classified S3, S4_ACE and S4_UnACE (regions outside of the eddies in S4) into different water masses in the western and southeastern SCS (Fig. 1). A principal component analysis (PCA) was performed to segment the underway dataset based on biological and environment factors (Fig. 3). The first two principal components accounted for more than 60% of the total variation, with the first principal component driven by variations in temperature and chlorophyll fluorescence and the second by SLA (Fig. 3). The groups distinguished based on chlorophyll fluorescence, SST and SLA accordingly separated within PC1-PC2 space.

3.1 The shelf edge of the northern SCS (Section S1)

Section S1 was located at the edge of the northern continental SCS shelf close to the Dongsha Atoll (Fig. 1). Section S1 had the lowest SST and highest Chla^{FRRf} of the survey (Fig. 2; Table 1). Ranges of SST and Chla^{FRRf} along this section varied from 26.7 – 28.0 ℃ and from 0.12 – 0.51 mg m^{-3}, respectively; but salinity showed small variability (33.4 – 33.76 *psu*; Figs. 2, 5). Phytoplankton compositions in this region were also distinct, with higher proportions of Prasinophytes (6-15%) ($p < 0.01$), Type-8 Haptophytes (9-19%) ($p < 0.01$), Diatoms (0-15%) ($p < 0.05$) and lower proportions of *Prochlorococcus* (18-30%) ($p < 0.05$) than the other sections (t-test for significantly different means; Fig. 4). Between stations C01 and C03, SST declined by ~0.8 ℃ and Chla^{FRRf} showed a synchronous peak (Fig. 5C). Although C03 was not at the center of SST minimum, Chla^{HPLC} was the highest observed (0.4 mg m^{-3}) and the diatom percentage contribution to total chlorophyll-a was also the highest for the cruise (15 %). Following C03, Chla^{HPLC} gradually decreased landwards whilst the proportions of Prasinophytes and Diatoms decreased but *Synechococcus* and *Prochlorococcus* increased (Fig. 4).

A peak of F_v/F_m up to 0.40 matched the SST minimum, closely corresponding with Chla^{FRRf} (Fig. 5C). Besides this peak, F_v/F_m values were relatively low (<0.3). The PSII functional absorption cross section (σ_{PSII}) remained relatively constant (mean of 701 Å²; Fig. 5C). Generally, F_v/F_m exhibited maxima at sunrise (~0.30) and sunset (~0.24) with depressions at midday (~0.20) and at about 22:00 (~0.27). By contrast, diel variability in σ_{PSII} (615 – 870 Å²) was relatively minor although demonstrated an afternoon increase (Fig. 5E).

3.2 The northern basin (Section S2)

Section S2 defined the 18 °N transect from 118 °E to 110 °E (Fig. 1). SLA showed higher values in the eastern part of the transect, contrasting with lower values around C21 (Fig. 1). SST between 28.7 and 30 ℃ was observed and increased gradually during the daytime in the area until reaching 114°E (Fig. 6). Salinity increased generally from 33.5 to 33.9 *psu* until a sharp drop to 33.3 *psu* before the station C21, and then a further reduction to 33.0 near Hainan Island (Figs. 2, 6B). Both Chla^{FRRf} (0.10 to 0.12 mg m^{-3}) and Chla^{HPLC} (~0.08 mg m^{-3}) were lower than S1 (Fig. 6C, Table 1) and phytoplankton compositions were *Synechococcus* (37-57%) and *Prochlorococcus* (32-51%) dominated (Fig. 4).

Compared with Section S1, F_v/F_m (0.10-0.30) and σ_{PSII} (416-799 Å²) values in S2 were significantly lower ($p < 0.01$) (Table 1). However, the fluctuation of diel patterns of F_v/F_m in S2 were more pronounced, showing lower peaks at sunrise (~0.27) and sunset (~0.23) and pronounced midday (~0.14) and more modest night time (~0.20) reductions (Fig. 6D). Furthermore, σ_{PSII} showed a clear

diel pattern, with a pronounced midday maximum that was around 1.4-fold higher than night time values (Fig. 6E).

3.3 The eddy domain of the western SCS (Section S3)

Section S3 started from Hainan Island heading southeast, intersecting the edge of a cyclonic eddy to the east of Vietnam (Fig. 1). Along this section SLA were depressed (-0.07 - 0.13 m) and within the vicinity of the cyclonic eddy SST ranged 29.3–30 °C (Table 1; Fig. 7B). Chla^{FRRf} remained relatively constant (~0.10 mg m^{-3}) (Fig. 7C; HPLC samples not collected).

Values of F_v/F_m were significantly higher than S2 and S4 ($p < 0.01$), varying between 0.14–0.32 in the cyclonic eddy (Table 1). F_v/F_m showed a clear diel pattern, with higher sunrise (~0.29), sunset (~0.29), and lower midday (~0.17) and night (~0.23) values (Fig. 7D, Table 1). Values of σ_{PSII} remained relatively constant (421- 587 Å²) in the cyclonic eddy, with a small increase around midday (Fig. 7E).

3.4 The southeastern basin (Section S4)

This section intersected anticyclonic eddies ACE1 and ACE2 (S4_ACE) with regions outside of the eddies defined as S4_UnACE (Fig. 1). Salinity varied between 32.0 and 33.3 *psu*, and SST between 29.2 and 30.6 °C. The map showed this section, particularly outside the ACEs, was characterized by the lowest salinity among all sections (Fig. 2B). Chla^{FRRf} remained relatively constant (0.11 - 0.12 mg m^{-3}) but increased (~0.14 mg m^{-3}) on the outside of ACE1 associated with a salinity decrease (~32.0 *psu*). Two abrupt changes in Chla^{FRRf} were observed at the edge of ACEs, with Chla^{FRRf} increasing by ~0.03 mg m^{-3}. Across ACE2 SST and salinity was relatively constant (29.3-29.7 °C; salinity ~33.1 *psu*), whilst Chla^{FRRf} gradually declined from 0.14 to 0.10 mg m^{-3} (Fig. 8). *Synechococcus* and *Prochlorococcus* together were the largest contributor to Chl*a* throughout (Fig. 4).

Ranges of F_v/F_m inside and outside the ACEs were 0.07 – 0.26 and 0.07 – 0.32, respectively. Smoothed F_v/F_m curves showed the sunrise (~0.19) and sunset values (~0.17) inside the ACEs were similar with those outside (~0.21 and ~0.19), but those curves overlooked spatial variations, for example, the ACE1 had apparent higher sunrise and sunset F_v/F_m than the ACE2; nevertheless, the smoothed curves did capture the midday minimum (0.09±0.01) inside the ACEs which was lower than those outside (0.13±0.04) (Fig. 8D, Table 1). The values of σ_{PSII} were the lowest of the cruise and varied between 64 and 663 Å² (Table 1), and the diel patterns showed a small increase of σ_{PSII} in the afternoon both inside and outside ACEs (Fig. 8E).

3.5 Comparisons between and within sections

Section S1 was distinct to other sections and characterized by lower SST of 27.4±0.3 °C and higher Chla^{FRRf} of 0.24±0.10 mg m^{-3} (Table 1). Section S1 was heterogeneous with the abrupt bump of F_v/F_m at the first night (Fig. 5). Sections S2 and S3 were relatively homogenous, F_v/F_m were consistently higher in Section S3 than those in Section S2, although the differences were quantitatively small (Table 1). Moreover, σ_{PSII} in Section S2 had a significant increase in the afternoon which was not apparent in Section S3 (Fig. 6). The average dawn F_v/F_m of sections S1-3 were all smaller than 0.3 (0.26-0.29) but still higher than that in Section S4 (0.18 and 0.21 inside and outside ACEs, respectively). Corresponding to similar iPAR at noon, ACEs revealed significantly lower noon F_v/F_m (0.09±0.01) than that of S4_UnACE. In general, F_v/F_m experienced less than 20% reduction at midnight but up to 50% at noon, by using the dawn value as the reference.

4 Discussion

Our results of the active fluorescence measurements in the SCS may reflect diurnal variations in FRRF-derived parameters as well as spatial changes in photo-physiology of phytoplankton assemblages and their taxonomic compositions related to environmental forcing (Behrenfeld et al., 2006; Suggett et al., 2009). Therefore, it was challenging to compare any instantaneous F_v/F_m measurement between regions (Fig. S2). We first discuss the influence of phytoplankton composition on FRRF-derived parameters and typical diurnal patterns over the entire SCS, followed by a discussion on effects of mesoscale eddy structure on phytoplankton photo-physiology within the SCS.

4.1 Challenge 1: understudied photophysiology of prokaryotic phytoplankton

Suggett et al. (2009) showed from active fluorescence data for phytoplankton cultures in previous studies that there was a negative relationship between (optimal) F_v/F_m and σ_{PSII} across eukaryotic taxa. The relationship was explained by the distinct light absorption and excitation energy transfer for each taxon and their energetic interpretation, which were likely related to selective pressure during phytoplankton evolution. However, in this study, no relationship was found between the two measurements (Fig. 9A) despite bulk σ_{PSII} actually reflected the relative amount of light-harvesting pigments (which was governed by phytoplankton composition) (Figs. 9B and 9C). Assuming that F_v/F_m of eukaryotic phytoplankton in the SCS was also taxonomic-dependent, perhaps the lack of a negative relationship was due to the contribution by both FRRF parameters from *Synechococcus* predominated in the SCS surface waters. This is because *Synechococcus* have relatively low σ_{PSII} (at blue excitation waveband) and F_v/F_m, attributed to their light absorption maxima more shifted to 'green' and the fluorescence from their relatively abundant PSI and phycocyanin which disturbs PSII fluorescence signal (Raateoja et al., 2004). On the other hand, *Prochlorococcus*, another dominant species of SCS, has been reported to have different F_v/F_m and σ_{PSII} than *Synechococcus* (Raateoja et al., 2004; Six et al., 2007; Suggett et al. 2009), probably due to distinct pigment compositions with predominantly divinyl chlorophyll (Ting et al., 2002). In any case, the lack of a negative F_v/F_m versus σ_{PSII} relationship as expected from taxonomic changes for eukaryotic phytoplankton, was partly due to the dominance of *Synechococcus*, whose parameters do not follow it.

Meanwhile, the low drawn F_v/F_m below 0.3 may be related to the dominance of *Synechococcus*. This is because *Synechococcus* are known to overexpress iron stress-induced chlorophyll binding protein IsiA under Fe-limited conditions, whereby the extra fluorescence from the IsiA supercomplexes detached to reaction centers would reduce apparent F_v/F_m (Schrader et al., 2011). Antenna proteins similar with IsiA are also found in low-light ecotypes of *Prochorococcus* (Bibby et al., 2003). However, this hypothesis of Fe deficiency in surface waters of the SCS basin appears unlikely as the measured nitrate concentration were 0.002-0.2 μM and previously reported Fe concentrations for this region were 0.2-0.3 nM (Wu et al., 2003; Wen et al., 2022), by assuming a threshold of 10:1 N:Fe ratio (μM:nm) for Fe limitation (Browning et al., 2017). Perhaps more likely is that absolute values of F_v/F_m are influenced by the active fluorescence measurement protocol as well as the instrument used and as such should be evaluated with caution (as discussed in section 4.2).

4.2 Challenge 2: widespread diel pattern of F_v/F_m throughout the SCS

Diel variability of F_v/F_m was observed throughout the SCS, with midday minima, maxima at dawn and dusk, and a slight nocturnal decrease (Figs. 5-8). This pattern has been observed previously in the central SCS (Xie et al., 2018) and the coastal SCS (Xu et al., 2020; Mai et al., 2021) and several other studies elsewhere in the tropical ocean (Behrenfeld et al., 2006; Doblin et al., 2011; Mackey et

al., 2008; Browning et al., 2017). The magnitude of midday minima can vary with incident PAR at noon as well as the duration of dark acclimation. In this study, the 5-minute dark acclimation did not provide sufficient time for phytoplankton to relax the slow NPQ components which could last for tens of minutes to hours. Furthermore, any repair of damaged PSII reaction centers also requires longer timescales. The sustained quenching to chlorophyll fluorescence led to a lower dark-acclimated F_m and F_v/F_m than it would be with a longer dark acclimation timescale (Fig. S3). The decline in F_v/F_m relative to its dawn value was positively correlated with the incident PAR (Fig. S4), suggesting the photoprotective nature of NPQ.

In general, it is expected that the nocturnal reduction of F_v/F_m is due to PQ pool reduction by 'chloro-respiration' in dark and is thought to depend on the degree of Fe stress that would deplete photosynthetic components (such as cytochrome b6f and photosystem I (PSI)) on the accepter side of the electron transfer chain (Behrenfeld and Milligan, 2013). The nocturnal reduction in the SCS was up to ~20% (in Section S4) is smaller than the nocturnal reduction of >25% seen in Fe limited surface waters in the equatorial Pacific reported by Behrenfeld et al. (2006). This may suggest that phytoplankton growth in the SCS was not severely Fe limited. Behrenfeld et al. (2006) also used dawn F_v/F_m maxima in combination with nocturnal reduction to delineate three ecophysiological regimes in the tropical Pacific (iron-sufficient with low macronutrients, iron-limited with low macronutrients, and iron-limited with elevated macronutrients). Following their diagnostic diagram (Fig. 4 in Behrenfeld et al. (2006)), our SCS data did not belong to any of those three since dawn F_v/F_m was less than 0.45. While this could imply a substantial difference between the tropical Pacific and the SCS with respect to nutrient availability, such comparisons should be made with caution. This is because absolute values of F_v/F_m are highly dependent on active fluorescence measurement protocols and employed instrumentation. For example, our correction using blank fluorescence from deionized water instead of filtered seawater might have underestimated F_v/F_m measurements (Cullen and Davis, 2003). If the underestimation of F_v/F_m in this study was true, the categorization of the SCS should possibly be the regime "iron-sufficient with low macronutrients", consistent with the reported Fe and nitrate data in the SCS waters in literatures (Wu et al., 2003; Wen et al., 2022). Such speculation should be examined in future nutrient addition experiments.

4.3 Nutrient effects on phytoplankton physiology by cyclonic eddies

Nutrients are usually considered as the most important factor for the growth of phytoplankton in the SCS (Ho et al., 2015), and always depleted in the upper mixed layer in the oligotrophic water along with strong stratification during summer. In this study, as described above, F_v/F_m at surface was typically as low as 0.1 – 0.3, and phytoplankton communities were dominated by *Synechococcus* and *Prochlorococcus* at the surface, indicating the oligotrophic condition in most of our study area during this cruise. Within the study area, it is expected that section S3 region crossing the cyclonic eddy was pumped with some nutrients from the nutrient-rich deeper layer (McGillicuddy, 2016), and therefore, phytoplankton physiological status may have been more favorable. The F_v/F_m exhibited consistently higher values in Section S3 where CE occurred than in the preceding Section S2 ($p < 0.01$) (Fig. 7; Table 1), but the increases (about 0.04) were small, and the diel variation remained the same (Figs. 6 and 7). The high SST of 29.5 – 30 °C likely rejected the assumption of large amount of nutrient-rich water injected into the surface. At the same time, the Chla^{FRRf} values in Section S3 were about 0.11 mg m^{-3}, as similar as that in Section S2. Previous studies in the SCS showed both elevated nutrient inventory and Chl*a* in CE, but cold and nutrient-rich water injected mainly into the lower part of euphotic zone; Chl*a* at the deep chlorophyll maximum layer could be increased to larger than 1 mg m^{-3} which was more than double of the background concentration, but Chl*a* at surface was rarely increased, the reported surface Chl*a* within cold eddies (normally 0.1 – 0.2 mg m^{-3}) was consistent

with our observation (Jiao et al., 2014; Liao et al., 2021; Wang et al., 2016). Taken together, these results implied that the CE had limited impacts on the surface phytoplankton communities. On the contrary, small scale but large increases in F_v/F_m were observed in the shelf area. Section S1 adjoined the Dongsha Atoll, where internal waves were frequently detected (Hsu et al., 2000; Liu et al., 2006; Pan et al., 2012; Zhao et al., 2004) (Fig. 1). The sudden drop of SST value, corresponding the higher Chla^{FRRf} than those in nearby subregion in this area, consisted with previous studies and indicated the occurrence of the internal waves between the station C01 and C03 along this transect (Figs. 2, 5). The dawn F_v/F_m of as high as 0.4 was accompanied by a Chl*a* concentration of about 0.4 mg m^{-3} and 15% contribution by diatoms at station C03. The results suggested that the F_v/F_m pattern observed in Section S1 was significantly affected by physical processes that can effectively supply nutrients to fuel phytoplankton growth. It also suggests that this level of nutrient supply cannot be reproduced by physical processes associated with the mesoscale cyclonic eddy structure seen in section S3. However, it should be noted that the change in F_v/F_m is usually disproportional to the change in carbon fixation; a study in the CE area of the western SCS but half month before this study found a twofold increase in the average Chl*a*-specific carbon fixation rate inside the CE than outside (Liao et al., 2021), with the implication being that FRRF could not probe any altered photosynthetic efficiency that dose not occur at the intracellular site of PSII.

4.4 Effects of anticyclonic eddies on phytoplankton physiology

The lowest values of F_v/F_m were found in the southeast basin associated with the ACE2 (Fig. 8), these may be explained in the case of that anticyclonic eddy based on the doming of its isopycnals and nutricline, therefore, lower sustained phytoplankton biomass in this area (McGillicuddy, 2016). ACE1 was adjacent to the Mekong River plume area characterized by lower salinity of < 32.5 *psu* while the ACE2 located in the remote and more oligotrophic southeast basin. The river input provides nutrients to promote phytoplankton growth and the dawn F_v/F_m in ACE1 was 0.24 (Fig. 8D). Meanwhile, the ACE2 showed the lowest Chl*a* of 0.07 mg m^{-3} corresponding to a dawn F_v/F_m of 0.17. Huang et al. (2010) reported two ACEs in the northern SCS during wintertime with much more abundant eukaryotic phytoplankton in the ACE with entrainment of coastal water. These phenomena highlighted the effects of source water mass on phytoplankton in ACEs. But the midday minimums of F_v/F_m were the same (~0.09) between the two ACEs (Fig. 8D) with the phytoplankton in the ACE1 exhibiting higher light sensitivity than those in surrounding waters.

5 Conclusions

In this study, underway FRRf measurements were used to record high resolution diel changes in F_v/F_m and σ_{PSII} throughout the SCS. Pronounced diurnal variability of both F_v/F_m and σ_{PSII} were observed, characterized by large midday depressions and slight nocturnal depressions of F_v/F_m, and slight increases in σ_{PSII} at noon, which was especially pronounced under expected elevated nutrient stress conditions. Slightly but consistently higher F_v/F_m throughout the day in the western SCS compared to the northern SCS basin suggested the potential role of cyclonic eddies in partially relieving nutrient stress. Apparent increase in F_v/F_m occurred only in a shelf area influenced by internal waves, where we hypothesize nutrients were injected into surface waters. The two ACEs exhibited different dawn, dusk, and night time values of F_v/F_m, indicating effects of source water mass on phytoplankton photophysiology. We recommend that future studies investigating phytoplankton photophysiology in the SCS should focus on more detailed mechanisms (e.g. vertical structure of mesoscale eddies, any other mesoscale process, typhoon) possibly via nutrient addition experiments conducted over different timescales to directly test the impact of nutrient supply on phytoplankton photophysiology.

390

391 **Figure Legends**

392 Figure 1: Map of sampling stations based on the average sea level anomaly (SLA) from 2018/09/18
393 to 2018/10/14. The top-left box indicates the matched daily sea level anomaly (SLA) of the cruise
394 track. The black dots were stations with phytoplankton pigment survey during the cruise. The color
395 lines were the cruise track which can be divided into 4 transects: S1 was selected as the continental
396 shelf of northern SCS; S2 referred to the basin of northern SCS; S3 located in the western SCS where
397 cyclonic eddies occurred; S4 distributed in the basin of southeastern SCS. CE = cyclonic eddy; ACE
398 = anticyclonic eddy; The S1, S2, S3, S4_ACE (through ACE1 and ACE2) and S4_UnACE (outside
399 ACE1 and ACE2) were in green, red, blue, purple and grey, respectively.

400 Figure 2. Underway surface sea temperature (SST) **(A)**, surface salinity **(B)** and surface fluorescence
401 (Chla^{FRRf}) **(C)** during the cruise.

402 Figure 3. Principle component analysis (PCA) of matched underway biological and environment
403 factors during the cruise. The S1, S2, S3, S4_ACE (through ACE1 and ACE2) and S4_UnACE
404 (outside ACE1 and ACE2) were dots in green, red, blue, purple and grey, respectively.

405 Figure 4. The concentration of total Chl *a* (Chla^{HPLC}) and contributions of different phytoplankton
406 group during the cruise. Dino, Diat, Hap_8, Hap_6, Chlo, Cryp, *Proc*, *Syne*, and Pras are the
407 abbreviations for Dinoflagellates, Diatoms, Haptophytes (type 8), Haptophytes (type 6),
408 Chlorophytes, Cryptophytes, *Synechococcus*, *Prochlorococcus* and Prasinophytes.

409 Figure 5. The incident irradiance **(A)**, environment conditions including SST and Salinity **(B)**, F_v/F_m,
410 σ_{PSII} and Chla^{FRRf} **(C)**, diel pattern of F_v/F_m **(D)** and diel pattern of σ_{PSII} **(E)** for continental shelf of
411 the northern SCS (Section S1). Light yellow, white and grey shaded area indicate the HPLC sample
412 station, local daytime and nighttime, respectively. The red lines in D and E are smoothed using the
413 loess method (span = 0.3), while the black lines represent the regression values ± SE.

414 Figure 6. Same as Fig. 5 but for basin of the northern SCS (Section S2).

415 Figure 7. Same as Fig. 5 but for eddy domains in the Western SCS (Section S3).

416 Figure 8. Same as Fig. 5 but for the basin of the southeast SCS (Section S4).

417 Figure 9. The relationship between F_v/F_m and σ_{PSII} **(A)**; σ_{PSII} and photosynthetic carotenoids (PSCs) /
418 TChl *a* **(B)**; σ_{PSII} and *Euk* / TChl a **(C).** The color represents the time period with the legend in panel
419 C. *Euk* was short for eukaryotic phytoplankton.

420 Table 1. Mean ± SD of surface environment conditions and FRRf-derived parameters performance in
421 the SCS along the cruise. The superscript labels a,b,c and d implied significant difference at the level
422 of $p < 0.05$ using one-way ANOVA (SLA: sea level anomaly, PAR: daily integrated
423 photosynthetically available radiation at surface)

Location	Northern SCS		Western SCS	South Eastern SCS	
	Shelf (S1)	Basin (S2)	CE (S3)	ACE1&ACE2 (S4)	Outside ACE1&ACE2 (S4)

N	95	130	57	84	318
Temperature (°C)	27.38±0.28^{a}	29.32±0.28^{b}	29.68±0.17^{c}	29.53±0.26^{d}	29.66±0.28^{c}
Salinity (*psu*)	33.64±0.08^{a}	33.61±0.21^{a}	33.38±0.46^{b}	32.98±0.21^{c}	32.72±0.37^{d}
Chl*a*^{FRRf} (mg m^{-3})	0.24±0.10^{a}	0.11±0.01^{b}	0.11±0.01^{b}	0.11±0.01^{b}	0.11±0.01^{b}
SLA (m)	0.12±0.04^{a}	0.13±0.03^{a}	0.01±0.05^{b}	0.21±0.04^{c}	0.13±0.04^{a}
PAR (mol quanta m^{-2} d^{-1})	41.70±6.91^{a}	52.45±3.07^{b}	44.29±7.02^{a}	52.92±0.58^{b}	52.65±4.46^{b}
F_v/F_m	0.23±0.06^{a}	0.20±0.04^{b}	0.24±0.04^{a}	0.15±0.05^{c}	0.17±0.05^{d}
F_v/F_m *(T=dawn)*	0.29±0.07^{a}	0.26±0.03^{a}	0.27±0.03^{a}	0.18±0.04^{b}	0.21±0.05^{b}
F_v/F_m *(T=midnight)*	0.27±0.05^{a}	0.21±0.02^{b}	0.23±0.02^{ab}	0.16±0.04^{c}	0.17±0.04^{c}
F_v/F_m *(T=noon)*	0.17±0.05^{a}	0.14±0.02^{ab}	0.18±0.02^{a}	0.09±0.01^{c}	0.13±0.04^{b}
σ_{PSII} (Å²)	714±70^{a}	547±77^{b}	508±41^{c}	437±101^{d}	484±77^{c}

Data Availability Statement

The original contributions presented in the study are included in the article/supplementary material. Further inquiries can be directed to the corresponding author.

Conflict of Interest

The authors declare that the research was conducted in the absence of any commercial or financial relationships that could be construed as a potential conflict of interest.

Author Contributions

HL, YX and BH conceived this study. HL and FX conducted the sample collection and analysis. HL drafted the original manuscript. YX and TJB critically reviewed and edited the manuscript. All authors contributed to the article and approved the submitted version.

Funding

This work was supported by the National Natural Science Foundation of China through grants 42130401 and 42141002.

Acknowledgments

We thank Yin-Ning Zhang who is very gentle to lend us FastOcean plus FastAct, and Gai-Lian Li for her supports on cruise preparation. We also thank NSFC Shiptime SharingProject (41749906) for supporting the cruises by R/V Tan *Kah Kee* (Nos: NORC2018-06). We also thank the captain and crew of R/V Tan *Kah Kee* for their tremendous helps during the cruise.

References

Barlow, R., Stuart, V., Lutz, V., Sessions, H., Sathyendranath, S., Platt, T., et al. (2007). Seasonal pigment patterns of surface phytoplankton in the subtropical southern hemisphere. *Deep Sea Res. Part I* 54(10), 1687-1703. doi: 10.1016/j.dsr.2007.06.010

Behrenfeld, M. J., and Boss, E. (2006). Beam attenuation and chlorophyll concentration as alternative optical indices of phytoplankton biomass. *J. Mar. Res.* 64, 431-451. doi:

10.1357/002224006778189563
Behrenfeld, M.J. and Kolber, Z.S. (1999). Widespread iron limitation of phytoplankton in the south Pacific Ocean. *Science* 283(5403), 840-843. doi: 10.1126/science.283.5403.840
Behrenfeld, M.J. and Milligan, A.J. (2013). Photophysiological expressions of iron stress in phytoplankton. *Annu. Rev. Mar. Sci.* 5, 217-246. doi: 10.1146/annurev-marine-121211-172356
Behrenfeld, M.J., Worthington, K., Sherrell, R.M., Chavez, F.P., Strutton, P., McPhaden, M. and Shea, D.M. (2006). Controls on tropical Pacific Ocean productivity revealed through nutrient stress diagnostics. *Nature* 442(7106), 1025-1028. doi: 10.1038/nature05083
Bibby, T. S., Mary, I., Nield, J., Partensky, F., and Barber, J. (2003). Low-light-adapted Prochlorococcus species possess specific antennae for each photosystem. *Nature* 424, 1051–1054. doi: 10.1038/nature01933
Brewin, R.J.W., Sathyendranath, S., Jackson, T., Barlow, R., Brotas, V., Airs, R., Lamont, T. (2015). Influence of light in the mixed-layer on the parameters of a three-component model of phytoplankton size class. *Remote Sensing Environ.* 168, 437–450. doi: 10.1016/j.rse.2015.07.004
Browning, T. J., Bouman, H. A., Moore, C. M., Schlosser, C., Tarran, G. A., Woodward, E. M. S., et al. (2014). Nutrient regimes control phytoplankton ecophysiology in the South Atlantic. *Biogeosciences* 11, 463–479. doi: 10.5194/bg-11-463-2014
Campbell, D., Hurry, V., Clarke, A.K., Gustafsson, P. and Öquist, G. (1998). Chlorophyll Fluorescence Analysis of Cyanobacterial Photosynthesis and Acclimation. *Microbiol. Mol. Biol. Rev.* 62(3), 667-683. doi: 10.1128/MMBR.62.3.667-683.1998
Cullen, J.J., and Davis, R.F. (2003). The Blank Can Make a Big Difference in Oceanographic Measurements. Limnology and Oceanography Bulletin 12, 29-35.
Doblin, M. A., Petrou, K. L., Shelly, K., Westwood, K., van den Enden, R., Wright, S., et al. (2011). Diel variation of chlorophyll-a fluorescence, phytoplankton pigments and productivity in the Sub-Antarctic and Polar Front Zones south of Tasmania, Australia. *Deep Sea Res. Part II* 58, 2189–2199. doi: 10.1016/j.dsr2.2011.05.021
Falkowski, P.G., Barber, R.T. and Smetacek, V.V. (1998). Biogeochemical Controls and Feedbacks on Ocean Primary Production. *Science* 281(5374), 200-207. doi: 10.1126/science.281.5374.200
Falkowski, P.G., Ziemann, D., Kolber, Z. and Bienfang, P.K. (1991). Role of Eddy Pumping in Enhancing Primary Production in the Ocean. *Nature* 352(6330), 55-58. doi: 10.1038/352055a0
Field, C.B., Behrenfeld, M.J., Randerson, J.T. and Falkowski, P. (1998). Primary production of the biosphere: integrating terrestrial and oceanic components. *Science* 281(5374), 237-240. doi: 10.1126/science.281.5374.237
Furuya, K., Hayashi, M., Yabushita, Y. and Ishikawa, A. (2003). Phytoplankton dynamics in the East China Sea in spring and summer as revealed by HPLC-derived pigment signatures. *Deep Sea Res. Part II* 50(2), 367-387. doi: 0.1016/S0967-0645(02)00460-5
Hawco, N.J., Barone, B., Church, M.J., Babcock‐Adams, L., Repeta, D.J., Wear, E.K., Foreman, R.K., Björkman, K.M., Bent, S., Van Mooy, B.a.S., Sheyn, U., Delong, E.F., Acker, M., Kelly, R.L., Nelson, A., Ranieri, J., Clemente, T.M., Karl, D.M., and John, S.G. (2021). Iron Depletion in the Deep Chlorophyll Maximum: Mesoscale Eddies as Natural Iron Fertilization Experiments. *Global Biogeochemical Cycles* 35.
Ho, T.Y., Pan, X., Yang, H.H., George.T.F.W., Shiah, F.K. (2015). Controls on temporal and spatial variations of phytoplankton pigment distribution in the Northern South China Sea. *Deep Sea Res. Part II* 117, 65-85. doi: 10.1016/j.dsr2.2015.05.015
Holm-Hansen, O., Amos, A. F., and Hewes, C. D. (2000). Reliability of estimating chlorophyll-a concentrations in Antarctic waters by measurement of in situ chlorophyll-a fluorescence. *Mar. Ecol. Progr. Ser.* 196, 103-110. doi:10.3354/meps196103
Hsu, M.K., Liu, A.K. and Liu, C. (2000). A study of internal waves in the China Seas and Yellow Sea

using SAR. *Cont. Shelf Res.* 20(4-5), 389-410. doi: 10.1016/S0278-4343(99)00078-3

Huang, B.Q., Hu, J., Xu, H.Z., Cao, Z.R., Wang, D.X., (2010). Phytoplankton community at warm eddies in the northern South China Sea in winter 2003/2004. *Deep Sea Res. Part II* 57, 1792–1798. doi: 10.1016/j.dsr2.2010.04.005

Hughes, D.J., Campbell, D.A., Doblin, M.A., Kromkamp, J.C., Lawrenz, E., Moore, C.M. et al. (2018). Roadmaps and Detours: Active Chlorophyll-a Assessments of Primary Productivity Across Marine and Freshwater Systems. *Environ. Sci. Technol.* 52(21), 12039-12054. doi: 10.1021/acs.est.8b03488

Jiao, N., Zhang, Y., Zhou, K., Li, Q., Dai, M., Liu, J., Guo, J. and Huang, B. (2014) Revisiting the CO2 "sourcce" problem in upwelling areas – a comparative study on eddy upwellings in the South China Sea. *Biogeosciences* 11(9), 2465-2475. doi: 10.5194/bg-11-2465-2014

Jin, P., Gao, G., Liu, X., Li, F., Tong, S., Ding, J. et al. (2016). Contrasting Photophysiological Characteristics of Phytoplankton Assemblages in the Northern South China Sea. *PloS One* 11(5), e0153555. doi: 10.1371/journal.pone.0153555

Kolber, Z.S., and Falkowski, P.G. (1993). Use of Active Fluorescence to Estimate Phytoplankton Photosynthesis in-Situ. *Limnol. Oceanogr.* 38(8), 1646-1665. doi: 10.4319/lo.1993.38.8.1646

Kolber, Z.S., Prasil, O. and Falkowski, P.G. (1998). Measurements of variable chlorophyll fluorescence using fast repetition rate techniques: defining methodology and experimental protocols. *Biochim. Biophys. Acta Bioenerget.* 1367, 88-106. doi: 10.1016/s0005-2728(98)00135-2

Kromkamp, J.C., and Forster, R.M. (2003). The use of variable fluorescence measurements in aquatic ecosystems: differences between multiple and single turnover measuring protocols and suggested terminology. European Journal of Phycology 38, 103-112.

Latasa, M., 2007. Improving estimations of phytoplankton class abundances using CHEMTAX. *Mar. Ecol. Prog. Ser.* 329, 13–21. doi:10.3354/meps329013

Li, H., Wiesner, M.G., Chen, J., Ling, Z., Zhang, J. and Ran, L. (2017) Long-term variation of mesopelagic biogenic flux in the central South China Sea: Impact of monsoonal seasonality and mesoscale eddy. *Deep Sea Res. Part I* 126, 62-72. doi: 10.1016/j.dsr.2017.05.012

Liao, J., Xu, J., Li, R., Shi, Z. (2021). Photosynthesis-Irradiance Response in the Eddy Dipole in the Western South China Sea. *J. Geophys. Res. Oceans* 126(5), e2020JC016986. doi: 10.1029/2020jc016986

Liu, C.T., Pinkel, R., Klymak, J., Hsu, M.K., Chen, H.W. and Villanoy, C. (2006). Nonlinear internal waves from the Luzon Strait. *Eos* 87(42), 449-451. doi: 10.1029/2006eo420002

Longhurst, A., Sathyendranath, S., Platt, T. and Caverhill, C. (1995). An Estimate of Global Primary Production in the Ocean from Satellite Radiometer Data. *J. Plankton Res.* 17(6), 1245-1271. doi: 10.1093/plankt/17.6.1245

Mackey, K.R.M., Paytan, A., Grossman, A.R. and Bailey, S. (2008). A photosynthetic strategy for coping in a high-light, low-nutrient environment. *Limnol. Oceanogr.* 53(3), 900-913. doi: 10.4319/lo.2008.53.3.0900

Mackey, M.D., Mackey, D.J., Higgins, H.W. and Wright, S.W. (1996). CHEMTAX – A program for estimating class abundances from chemical markers: Application to HPLC measurements of phytoplankton. *Mar. Ecol. Prog. Ser.* 144(1-3), 265-283. doi: 10.3354/meps144265

Mai, G., Song, X., Xia, X., Ma, Z., Tan, Y., and Li, G. (2021). Photosynthetic Characteristics of Smaller and Larger Cell Size-Fractioned Phytoplankton Assemblies in the Daya Bay, Northern South China Sea. *Microorganisms* 10. doi: 10.3390/microorganisms10010016

Mella-Flores, D., Six, C., Ratin, M., Partensky, F., Boutte, C., Le Corguillé, G., et al. (2012). Prochlorococcus and Synechococcus have evolved different adaptive mechanisms to cope with light and UV stress. *Front. Microbiol.* 3, 285. doi: 10.3389/fmicb.2012.00285

McGillicuddy, D.J. (2016). Mechanisms of Physical-Biological-Biogeochemical Interaction at the

Oceanic Mesoscale. *Annu. Rev. Mar. Sci.* 8(1), 125-59. doi: 10.1146/annurev-marine-010814-015606

Moore, C. M., Mills, M. M., Langlois, R., Milne, A., Achterberg, E.P., La Roche, J. et al. (2008). Relative influence of nitrogen and phosphorous availability on phytoplankton physiology and productivity in the oligotrophic sub-tropical North Atlantic Ocean. *Limnol. Oceanogr.* 53: 291–305. doi: 10.4319/lo.2008.53.1.0291

Moore, C. M., Mills, M. M., Arrigo, K. R., Berman-Frank, I., Bopp, L., Boyd, P. W., et al. (2013). Processes and patterns of oceanic nutrient limitation. *Nat. Geosci.* 6, 701–710. doi: 10.1038/ngeo1765

Ning, X., Chai, F., Xue, H., Cai, Y., Liu, C. and Shi, J. (2004). Physical-biological oceanographic coupling influencing phytoplankton and primary production in the South China Sea. *J. Geophys. Res. Oceans* 109(C10). doi: 10.1029/2004jc002365

Pan, X.J., Wong, G.T.F., Shiah, F.K. and Ho, T.Y. (2012). Enhancement of biological productivity by internal waves: observations in the summertime in the northern South China Sea. *J. Oceanogr.* 68(3), 427-437. doi: 10.1007/s10872-012-0107-y

Parkhill, J.-P., Maillet, G., and Cullen, J.J. (2001). Fluorescence-Based Maximal Quantum Yield for Psii as a Diagnostic of Nutrient Stress. *Journal of Phycology* 37**,** 517-529. doi: 10.1046/j.1529-8817.2001.037004517.x

R Development Core Team, 2016. R: a language and environment for statistical computing. Vienna, Austria: R Foundation for Statistical Computing. Open access available at: http://cran. R-project. Org.

Raateoja, Mika, Seppälä, Jukka, Ylöstalo, Pasi, (2004), Fast repetition rate fluorometry is not applicable to studies of filamentous cyanobacteria from the Baltic Sea, Limnology and Oceanography, 4, doi: 10.4319/lo.2004.49.4.1006

Schlitzer, R. (2019). Data Analysis and Visualization with Ocean Data View. https://odv.awi.de.

Schrader, P.S., Milligan, A.J., Behrenfeld, M.J. (2011). Surplus Photosynthetic Antennae Complexes Underlie Diagnostics of Iron Limitation in a Cyanobacterium. *PloS ONE* 6(4), e18753. doi: 10.1371/journal.pone.0018753

Schuback, N. and Tortell, P.D. (2019). Diurnal regulation of photosynthetic light absorption, electron transport and carbon fixation in two contrasting oceanic environments. *Biogeosciences* 16(7), 1381-1399. doi: 10.5194/bg-16-1381-2019

Six, C., Finkel, Z. V., Irwin, A. J., and Campbell, D. A. (2007). Light variability illuminates niche-partitioning among marine Picocyanobacteria. *PloS ONE* 2, e1341. doi: 10.1371/journal.pone.0001341

Suggett, D.J., Moore, C.M., Hickman, A.E. and Geider, R.J. (2009). Interpretation of fast repetition rate (FRR) fluorescence: signatures of phytoplankton community structure versus physiological state. *Mar. Ecol. Prog. Ser.* 376, 1-19. doi: 10.3354/meps07830

Ting, C.S., Rocap, G., King, J., and Chisholm, S.W. (2002). Cyanobacterial photosynthesis in the oceans: the origins and significance of divergent light-harvesting strategies. Trends in Microbiology 10, 134-142.

Wang, L., Huang, B. Q., Chiang, K.P., Liu, X., Chen, B.Z., Xie, Y. Y. et al. (2016). Physical-Biological Coupling in the Western South China Sea: The Response of Phytoplankton Community to a Mesoscale Cyclonic Eddy. *PLoS One* 11(4), e0153735. doi: 10.1371/journal.pone.0153735

Wang, L., Huang, B.Q., Laws, E.A., Zhou, K.B., Liu, X., Xie, Y.Y., Dai, M.H. (2018). Anticyclonic eddy edge effects on phytoplankton communities and particle export in the northern South China Sea. *J. Geophys. Res. Oceans* 123, 7632–7650. doi: 10.1029/2017jc013623

Wang, L., Huang, B., Liu, X., Xiao, W., 2015. The modification and optimizing of the CHEMTAX running in the South China Sea. *Acta Oceanol. Sin.* 34, 124–131. doi: 10.1007/s13131-015-0621-z

Wei, Y., Chen, Z., Guo, C., Zhong, Q., Wu, C., and Sun, J. (2020). Physiological and Ecological Responses of Photosynthetic Processes to Oceanic Properties and Phytoplankton Communities in the Oligotrophic Western Pacific Ocean. *Front Microbiol* 11, 1774.

Wen, Z., Browning, T.J., Cai, Y., Dai, R., Zhang, R., Du, C., Jiang, R., Lin, W., Liu, X., Cao, Z., Hong, H., Dai, M., and Shi, D. (2022). Nutrient regulation of biological nitrogen fixation across the tropical western North Pacific. Science Advances 8, eabl7564.

Wu, J., Chung, S.-W., Wen, L.-S., Liu, K.-K., Chen, Y.-L. L., Chen, H.-Y., et al. (2003). Dissolved inorganic phosphorus, dissolved iron, and *Trichodesmiumin* the oligotrophic South China Sea. Global Biogeochem. Cycles 17, 8-1–8-10. doi: 10.1029/2002gb001924

Xiao, W., Wang, L., Laws, E., Xie, Y., Chen, J., Liu, X., Chen, B., Huang, B. (2018). Realized niches explain spatial gradients in seasonal abundance of phytoplankton groups in the South China Sea. *Prog. Oceanogr.* 162, 223–239. doi: 10.1016/j.pocean.2018.03.008

Xie, Y., Laws, E.A., Yang, L. and Huang, B. (2018). Diel Patterns of Variable Fluorescence and Carbon Fixation of Picocyanobacteria Prochlorococcus-Dominated Phytoplankton in the South China Sea Basin. *Front. Microbiol.* 9, 1589. doi: 10.3389/fmicb.2018.01589

Xiu, P., Chai, F., Shi, L., Xue, H. and Chao, Y. (2010). A census of eddy activities in the South China Sea during 1993–2007. *J. Geophys. Res.* 115(C3). doi: 10.1029/2009jc005657

Xiu, P., and Chai, F. (2011). Modeled biogeochemical responses to mesoscale eddies in the South China Sea. *J. Geophys. Res.*116(C10). doi:10.1029/2010JC006800

Xu, K., Lavaud, J., Perkins, R., Austen, E., Bonnanfant, M., and Campbell, DA. (2018). Phytoplankton σPSII and Excitation Dissipation; Implications for Estimates of Primary Productivity. *Front. Mar. Sci.* 5:281. doi: 10.3389/fmars.2018.00281

Xu, G., Liu, J., Song, X., Tan, M., Ren, H., Li, D., Tan, Y., Huang, L., and Li, G. (2020). Diel Rhythm in Photosynthetic Performance of Phytoplankton Assemblages Is Predicted to Be Light-Dependent from in situ and Mesocosm Chlorophyll Fluorescence. *Journal of Coastal Research* 104.

Yi, X., Zhang, D., Sun, J., Beardall, J., Gao, K. (2021). Cyanobacteria-dominated phytoplankton in the oligotrophic South China Sea maintain photosynthetic potential despite diurnal photoinactivation of PSII. *Front. Mar. Sci.* 8:736586. doi: 10.3389/fmars.2021.736586

Zhang, M., Wu, Y., Wang, F., Xu, D., Liu, S., and Zhou, M. (2020). Hotspot of Organic Carbon Export Driven by Mesoscale Eddies in the Slope Region of the Northern South China Sea. *Front. Mar. Sci.* 7:444. doi: 10.3389/fmars.2020.00444

Zhao, Z.X., Klemas, V., Zheng, Q.N. and Yan, X.H. (2004). Remote sensing evidence for baroclinic tide origin of internal solitary waves in the northeastern South China Sea. *Geophys. Res. Lett.* 31(6). doi: 10.1029/2003gl019077

Zhu, Y., Feng, Y., Browning, T.J., Wen, Z., Hughes, D.J., Hao, Q., Zhang, R., Meng, Q., Wells, M.L., Jiang, Z., Dissanayake, P., Priyadarshani, W.N.C., Shou, L., Zeng, J., and Chai, F. (2022). Exploring Variability of Trichodesmium Photophysiology Using Multi-Excitation Wavelength Fast Repetition Rate Fluorometry. *Front Microbiol* 13, 813573.

Figure 1.JPEG

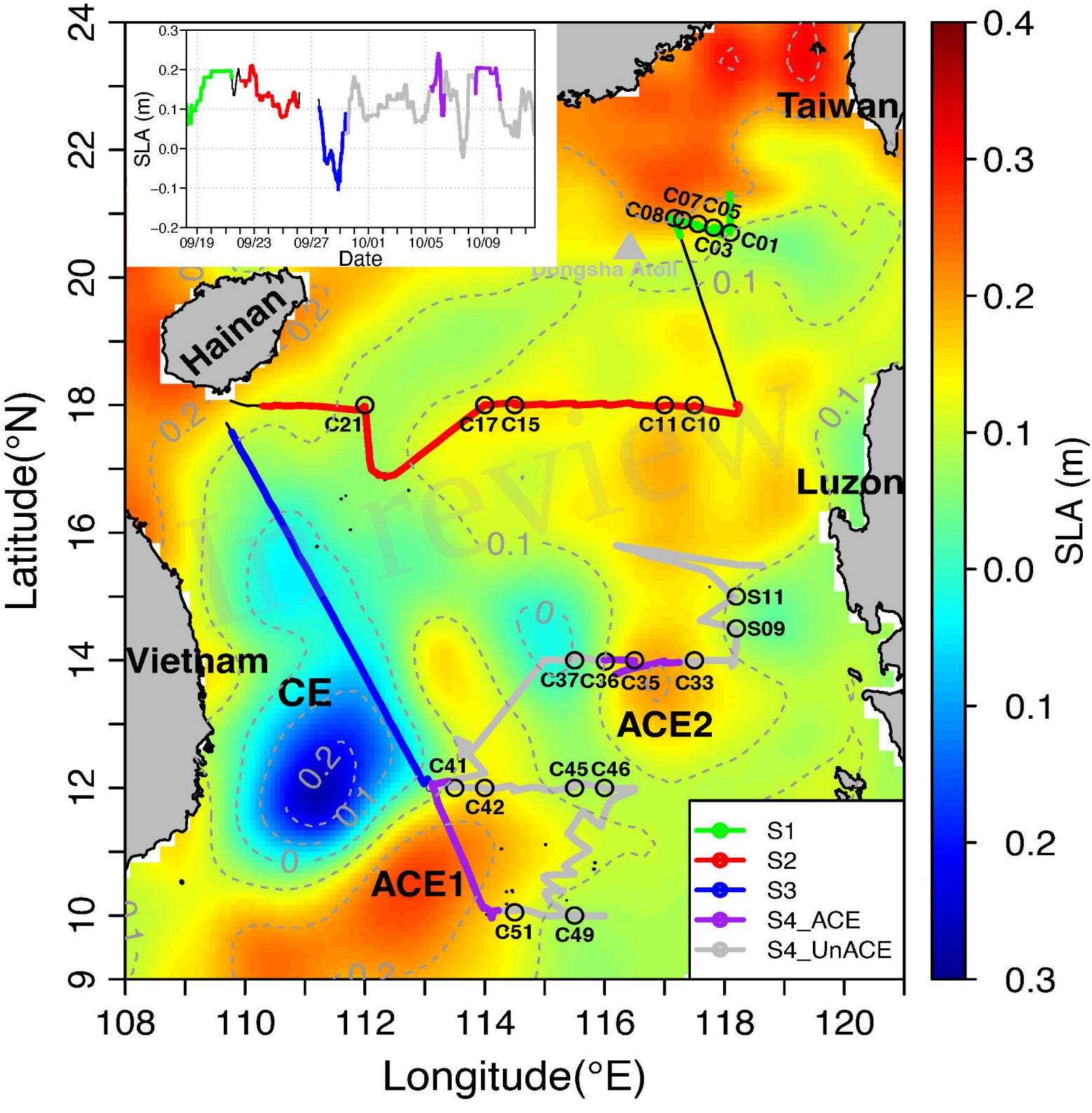

Figure 2.JPEG

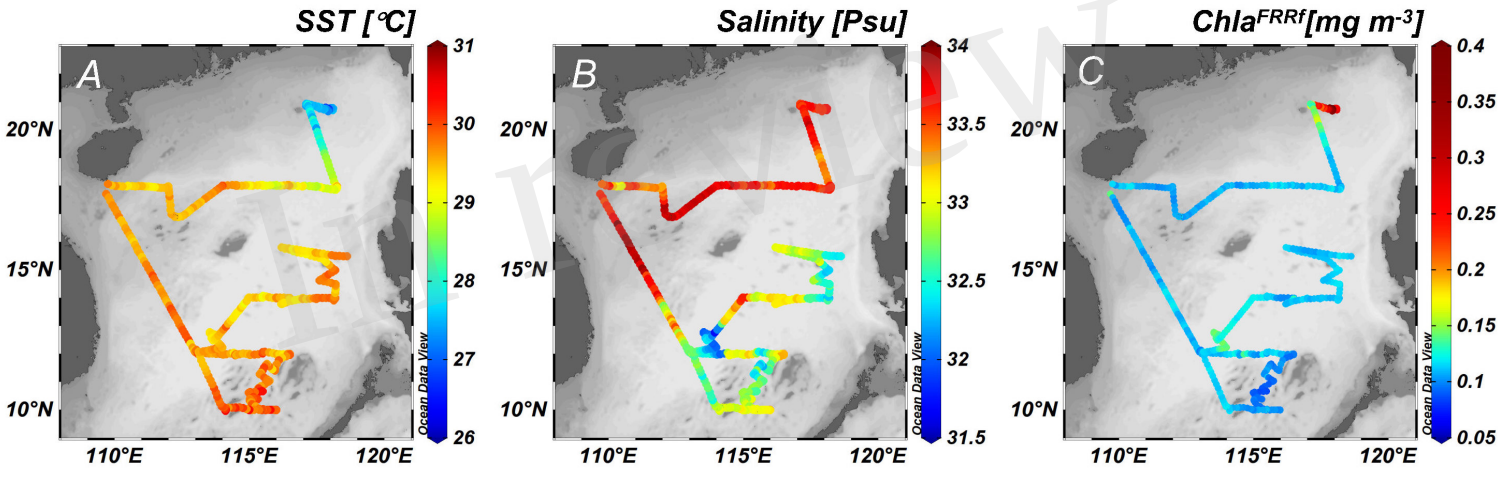

Figure 3.JPEG

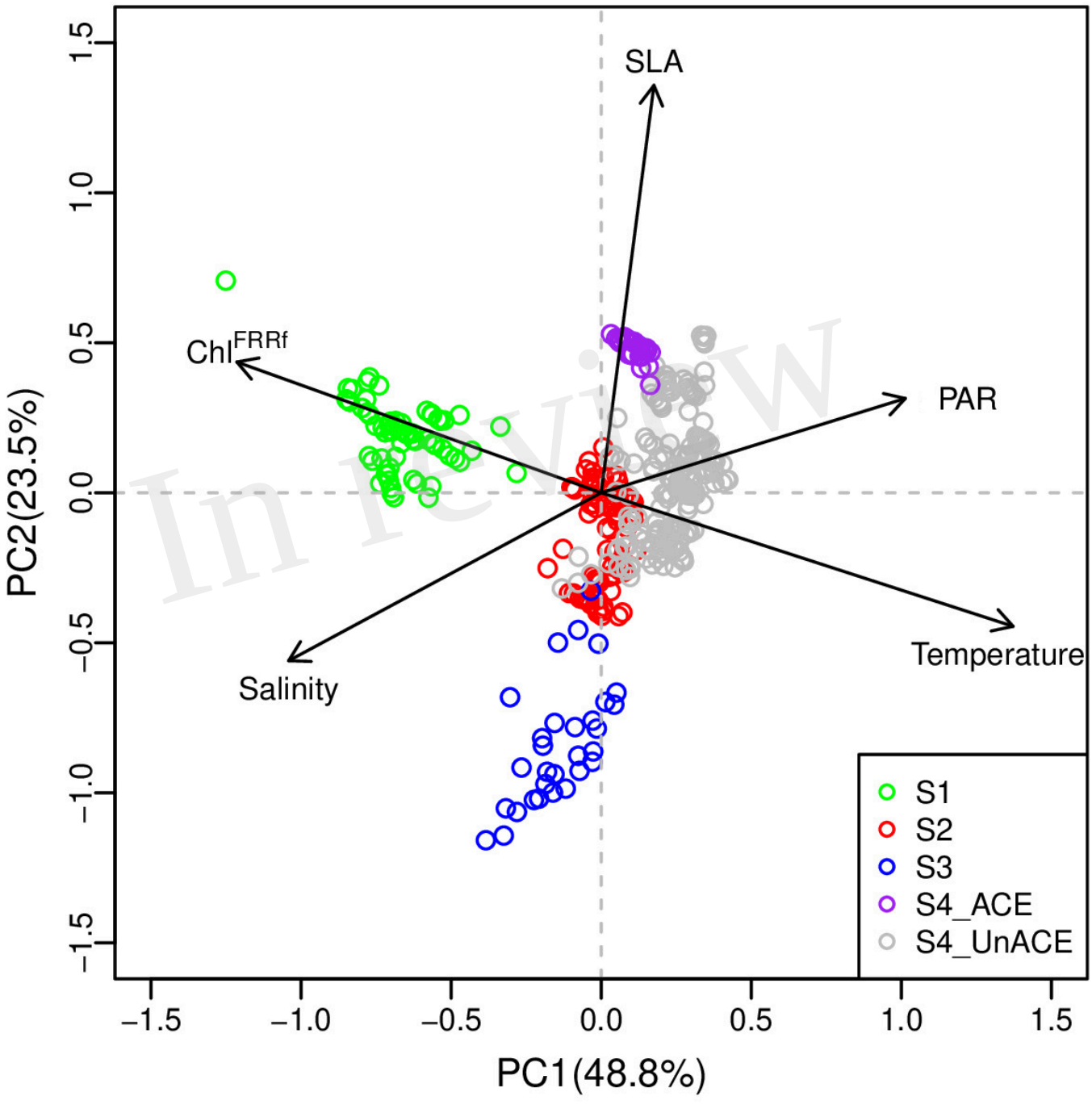

Figure 4.JPEG

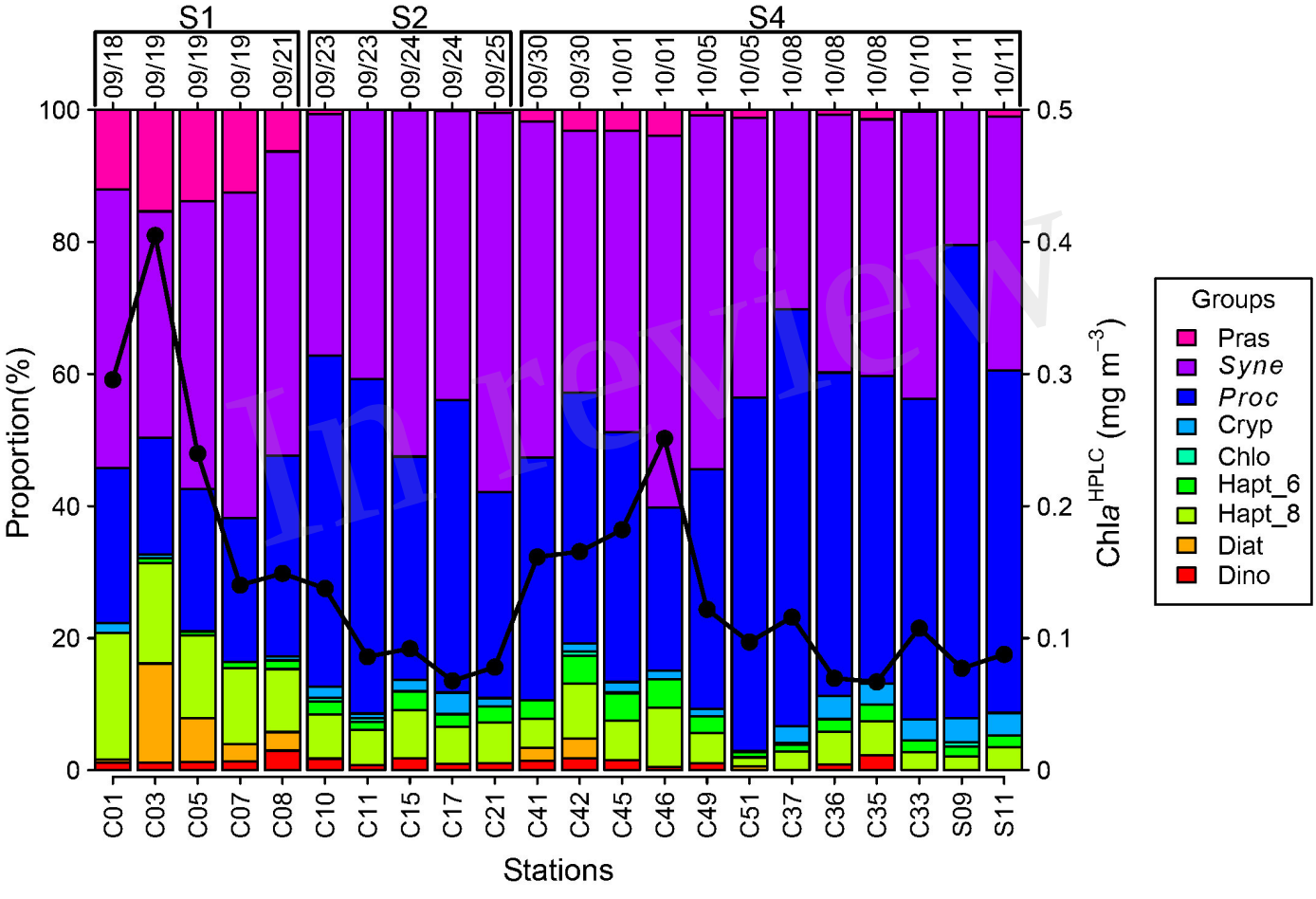

Figure 5.JPEG

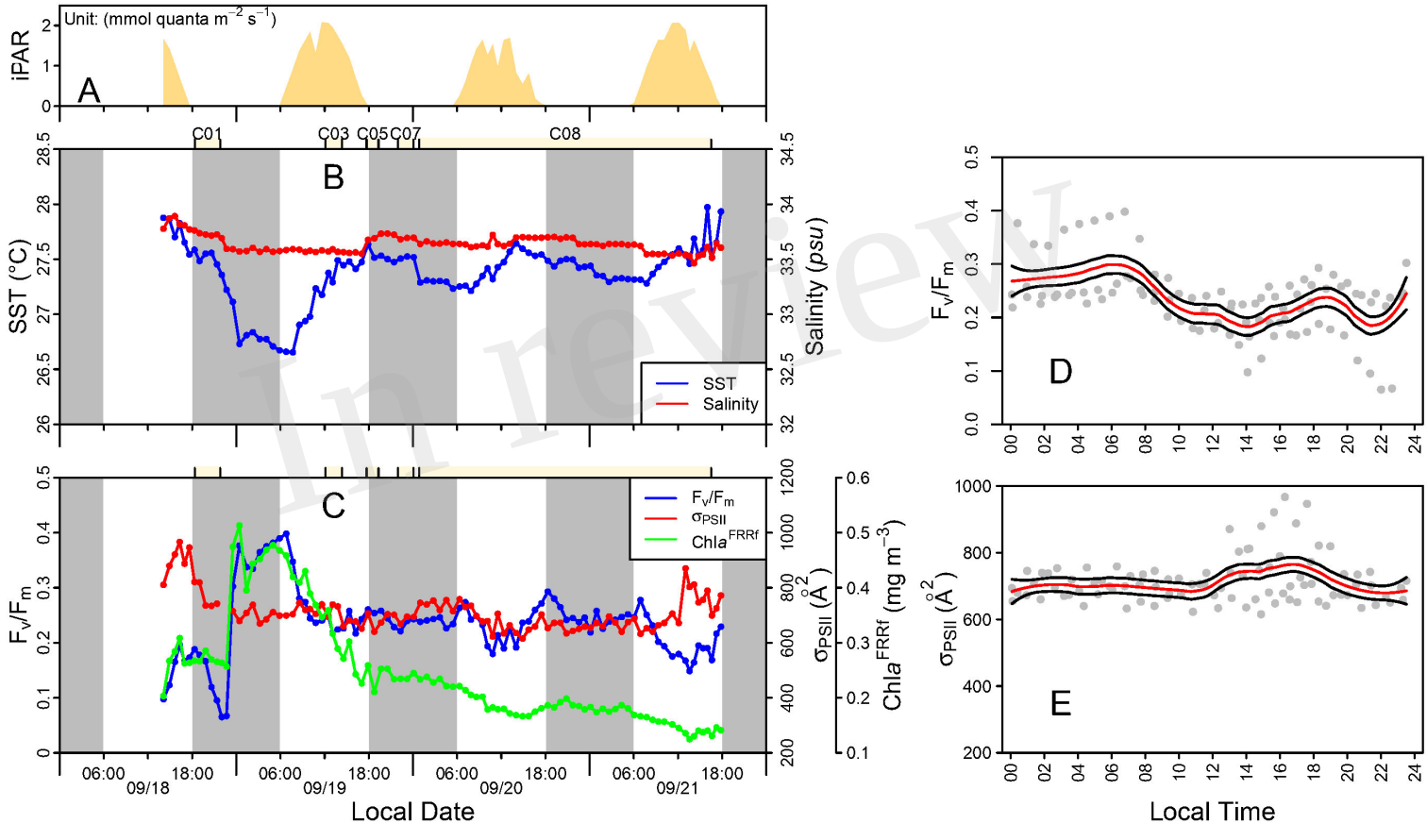

Figure 6.JPEG

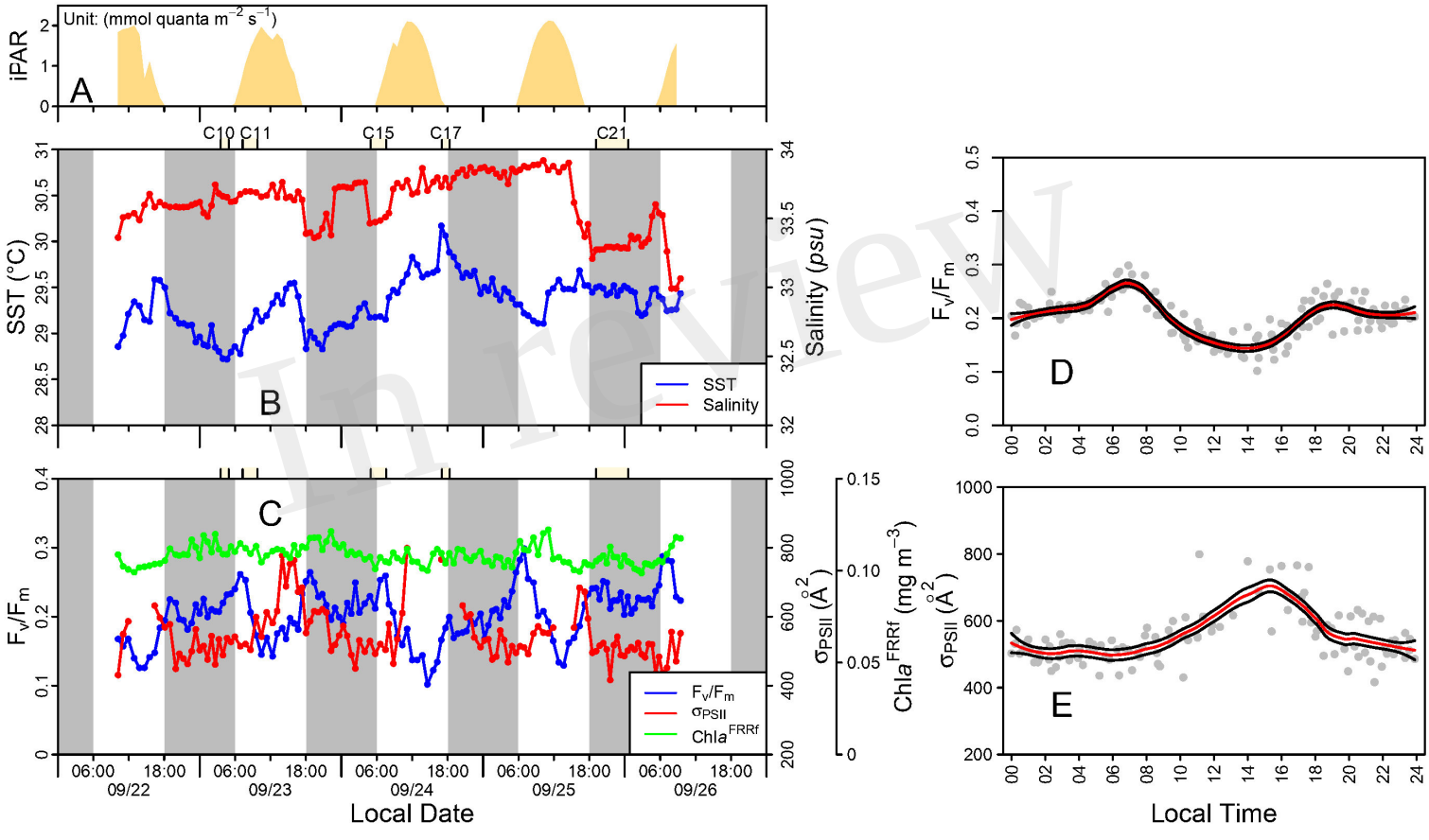

Figure 7.JPEG

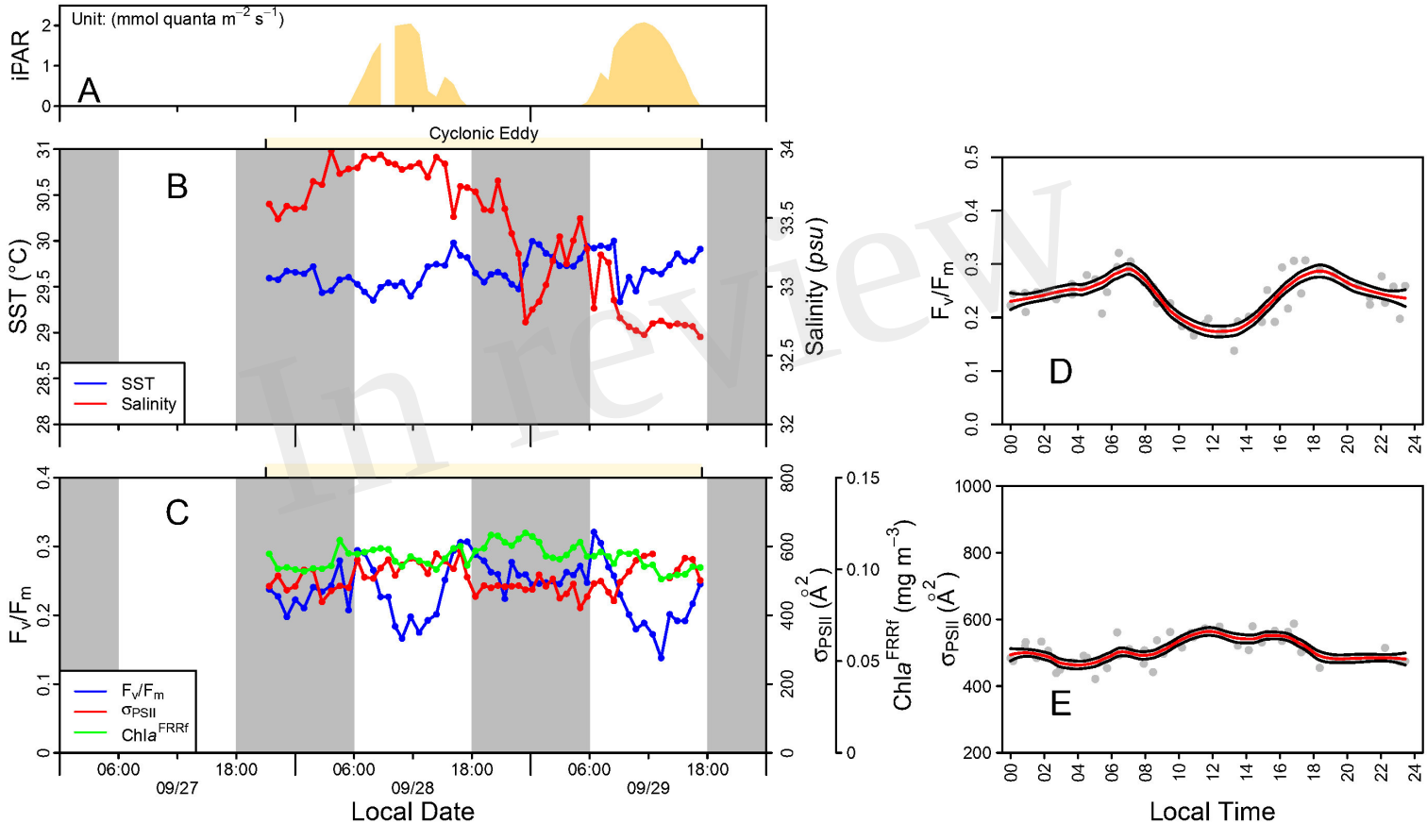

Figure 8.JPEG

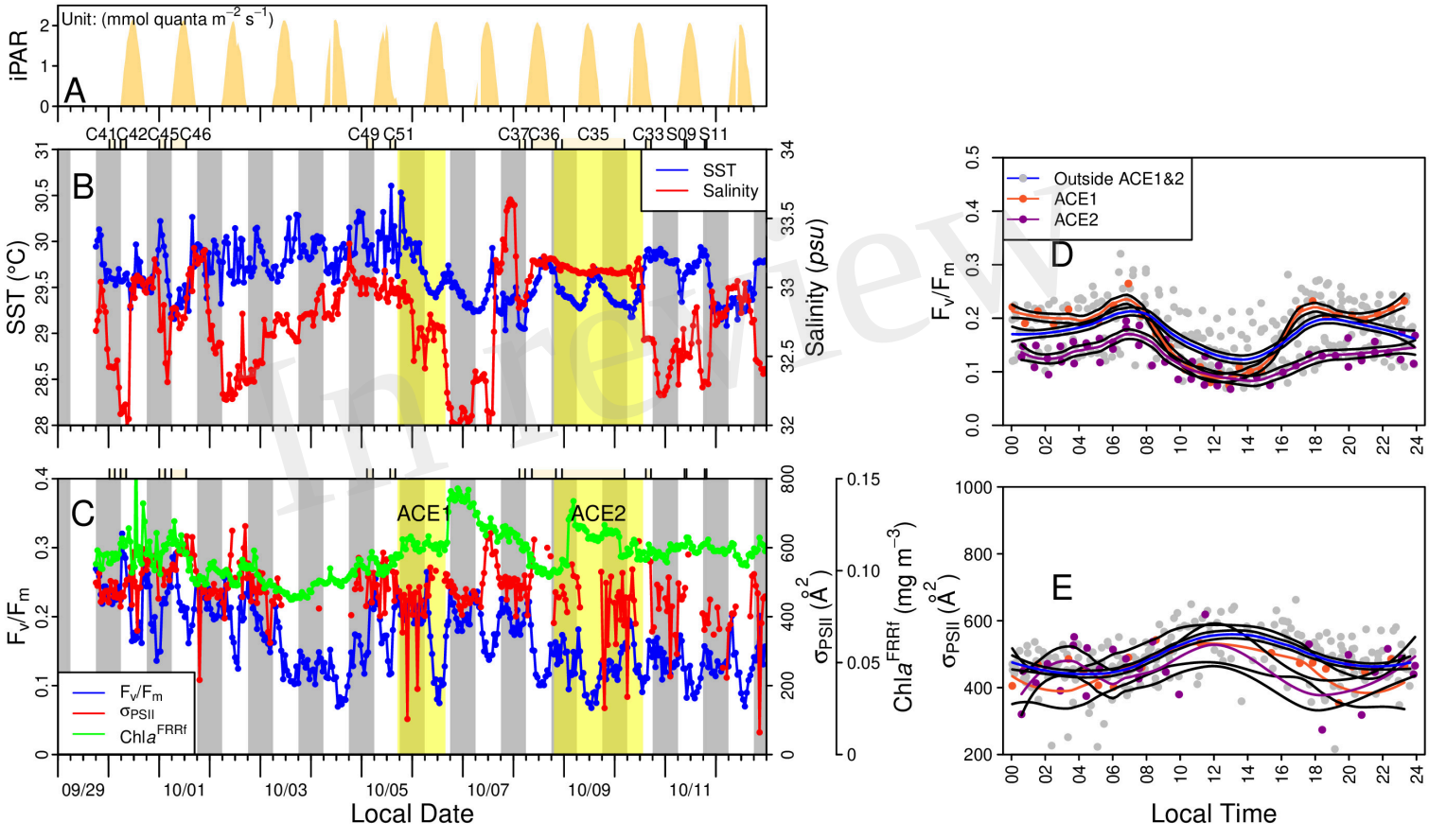

Figure 9.JPEG